symmetry

MDPI

Article

Research on Runway Capacity Evaluation of General Aviation Airport Based on Runway Expansion System

Zhiyuan Chen [1], Huachun Xiang [1,*], Bangcun Han [2], Yachen Shen [1], Ting Zhou [1] and Feng Zhang [1]

[1] Equipment Management and Unmanned Aerial Vehicle Engineering College, Air Force Engineering University, Xi'an 710051, China; czycc1993@163.com (Z.C.); shenyachen@eurasia.edu (Y.S.); ztpaper7625@163.com (T.Z.); peakerzhang@126.com (F.Z.)
[2] Shandong Airport Management Group Rizhao Airport Co., Ltd., Rizhao 276816, China; zsrz_hw@163.com
* Correspondence: xhc198036@163.com

Abstract: To enhance the operational management capabilities of general aviation airports, this paper proposes a method for evaluating the runway capacity of general aviation airports based on the runway expansion system. Firstly, it provides a brief introduction to the flight rules of general aviation airports and arrival and departure flight procedures with symmetrical characteristics, which serve as a theoretical basis for establishing the runway expansion system. Subsequently, a runway expansion system that covers symmetrical flight activities such as departure and arrival under a visual flight rule and an instrument flight rule is proposed, providing a conceptual model for evaluating the runway capacity of general aviation airports. On this foundation, the classical space–time analysis model is improved to establish a single runway arrival, departure, and mixed operation capacity evaluation model for general aviation airports. Finally, the reliability and rationality of this method are verified through case evaluations and three sets of numerical experiments with symmetrical relationships. The experiments demonstrate that this method can better reflect the actual conditions of the runways at general aviation airports while ensuring flight safety, and it can provide a reference for related research.

Keywords: runway expansion system; general aviation airport; runway capacity; visual flight rule; instrument flight rule

Citation: Chen, Z.; Xiang, H.; Han, B.; Shen, Y.; Zhou, T.; Zhang, F. Research on Runway Capacity Evaluation of General Aviation Airport Based on Runway Expansion System. *Symmetry* **2024**, *16*, 1555. https://doi.org/10.3390/sym16111555

Academic Editor: Hsien-Chung Wu

Received: 26 September 2024
Revised: 11 November 2024
Accepted: 18 November 2024
Published: 20 November 2024

1. Introduction

General aviation refers to civil aviation activities other than public air transportation. General aviation is known for its mobility, flexibility, speed, and efficiency. It encompasses a range of operations in low-altitude airspace, including agriculture, forestry, pastoralism, fisheries, transportation, sightseeing, photography, and rescue, making it an integral part of the modern comprehensive transportation system. According to the information publicly released in the "2023 Civil Aviation Industry Development Statistical Bulletin" by the Civil Aviation Administration of China, as of the end of 2023 [1], the total flight hours of general aviation in China reached 1.371 million, a 12.4% increase from 2022. The number of general aviation aircraft has reached 3303, and the number of general aviation airports has reached 449. It is evident that with the continuous development of general aviation in China and the ongoing refinement of low-altitude airspace management, the volume of general aviation flights is expected to grow rapidly. This growth not only promotes the prosperity of the industry but also brings pressure to the operational management of general aviation airports. Runways are critical for aircraft departure and arrival, directly affecting the upper limit of flight volume that an airport can handle. Limited by infrastructure constraints, the runway capacity of general aviation airports is finite. Faced with continuously increasing flight volumes, some airports are experiencing capacity bottlenecks and are even approaching saturation. In order to adapt to the development needs of general aviation and improve

operational efficiency, it is necessary to study the issue of runway capacity at general aviation airports.

Runway capacity assessment originated from the air traffic delay research conducted by American scholars Bowen and Pearcey in the 1940s [2]. Through continuous expansion by numerous scholars, it has now formed an airspace capacity assessment system that includes runway capacity assessment, airport capacity assessment [3], terminal area capacity assessment [4], air route capacity assessment [5], sector capacity assessment [6], and regional capacity assessment [7]. Correspondingly, the methods for capacity assessment have also been continuously enriched, evolving into a five-level assessment model [8], which includes the lookup table method, graphical method, mathematical analysis method, computer simulation method, airport capacity simulation model, and aircraft delay simulation model. The lookup table method is low in cost but less precise and is suitable for assessing the capacity of simple runways or airports. The mathematical analysis method and computer simulation method are simple in operation and have good scalability, making them suitable for assessing the capacity of runways and medium-sized airports. The airport capacity simulation model and aircraft delay model are high in precision but higher in cost and are suitable for assessing the capacity of complex airports, regions, and airspace systems.

Lookup table methods and chart methods primarily assess runway capacity based on historical statistical data, with the FAA AC 150/5060-5 [9] providing examples of their application. Mitkas [10] has proposed that for the capacity assessment needs of small general aviation airports, data collected via ADS-B, such as aircraft combinations and approach speeds, can be used to evaluate runway capacity. Additionally, these data can serve as initial inputs for other assessment models. Due to the inherent limitations of lookup table methods and chart methods, and the continuous enrichment and development of assessment methods, these techniques are currently often used as a verification method in runway capacity assessment. Farhadi [11] has calculated the runway capacity at Doha Airport using an improved heuristic algorithm, taking into account factors such as runway configuration, scheduling methods, and flight separation standards. By comparing with actual operational data from Doha Airport between 2007 and 2012, the method was found to provide the most accurate assessment results in multiple calculations. Ng [12] has researched how to increase runway capacity from the perspective of dynamic sequencing and scheduling in a semi-mixed operation mode. By testing and comparing with the actual operational data of Hong Kong International Airport from April 2018, the proposed method of dynamically adjusting the use of runways for aircraft takeoffs and landings was found to effectively enhance runway capacity.

The mathematical analysis method evaluates runway capacity based on mathematical equations constructed from factors related to runway capacity, and it may be combined with intelligent algorithms when necessary to improve computational power [13]. Donmez [14] started with the taxiway structure and established a runway capacity evaluation model based on runway occupancy time, average delay, and entry and exit points, studying the impact of three common taxiway configurations on capacity. Shen [15] started with the runway configuration and constructed a V-shaped open multi-runway capacity model based on the ELSO collision risk model, verifying the rationality of the model by substituting actual flight data. Based on the above research, Maltinti [16] optimized the taxiway exits under the guidelines of ICAO and FAA, and the demonstration results showed that this optimization significantly improved the airport's runway capacity. Gao [17] started with runway occupancy time and established a machine learning-based runway occupancy time prediction model, analyzing the factors affecting runway occupancy time and providing data support for air traffic controllers (ATCs) to adjust flight intervals and optimize runway taxiway design. Janic [18] started with air traffic control rules and proposed a new analytical model to study the runway arrival capacity problem of different aircraft combinations under various flight safety intervals. The experimental of this study indicates that runway capacity increases as the proportion of heavy aircraft in approach decreases, and vertical

separation can increase capacity more than horizontal separation. In addition to the above methods, there are also studies based on historical statistical data for constructing runway capacity evaluation models. For instance, Kim [19] preprocessed the historical statistical data in the ASPM database, selected key feature data that can affect the airport's runway capacity, and then used the censored regression model to operate on the new dataset to obtain the airport's runway capacity.

Computer simulation methods, airport capacity simulation models, and aircraft delay simulation models all use simulation software to mimic airport operations and assess runway capacity. Commonly used professional simulation software include AirTop [20], SIMMOD [21], and others. Tee [22] conducted a study on the dual runway capacity issue at Changi Airport using the AirTop simulation software. By simulating the flight activities of different types of aircraft during arrivals and departures, as well as runway operation scenarios, it was concluded that during non-peak airport operations, segregated parallel arrival–departure runway operations can better enhance runway capacity. During peak airport operations, using one of the runways exclusively for medium-sized aircraft can be more beneficial for increasing runway capacity. Cetek [23] built a rapid simulation model based on SIMMOD to study the runway capacity assessment issue at Ataturk Airport. By simulating airport operations during peak periods and runway maintenance scenarios, the optimal operation mode that can enhance runway capacity was determined. To reduce the cost of using the aforementioned specialized software, Yang [24] explored the application of Anylogic simulation software in runway capacity assessment and demonstrated the cost-effectiveness of the Anylogic software and the rationality of the experimental results by comparing them with the simulation outcomes of SIMMOD. Diaz [25] used system dynamics to study the impact of the continuous climb departure procedure on runway departure capacity. The research findings show that this procedure has a minor impact on departure capacity and can effectively reduce the workload of pilots and ATCs. Kaplan [26] used Monte Carlo simulation to assess the capacity of airports and their surrounding airspace. The experimental results indicate that the bottlenecks in air traffic flow at airports are often concentrated in the surrounding airspace, providing a reference for improving the operational management capabilities of relevant airports.

In addition to the methods mentioned above, Wan [27] constructed an airport environment traffic capacity assessment model based on big data from air traffic activities and conducted research on the capacity assessment of Nanjing Lukou International Airport. The results show that this model can accurately calculate the maximum hourly, daily, and annual capacities of Nanjing Lukou International Airport, providing a new idea and method for related research. Starita [28] considered the impact of uncertainties such as business aviation, weather, and military operations on airspace capacity assessments and established a mathematical model that takes into account both capacity assessments and management decision-making in stages, following the logic from airspace capacity determination to air traffic management. The capacity assessment data obtained through this model provide a decision-making reference for air traffic controllers to conditionally open sectors. Taking Starita's research approach as a reference, Kuennen [29] applied heuristic algorithms to the second-stage air traffic management model. The results of the case study indicate that in air traffic management, adopting a strategy of cross-border shared capacity can effectively increase air traffic flow and reduce operating costs.

In the face of the ever-increasing flight traffic, only by scientifically and accurately assessing the runway capacity of general aviation airports and providing solid data support for the operation and management of these airports can we ensure that general aviation airports continuously adapt to new development needs and maintain stable and efficient operations. Although the above research results provide valuable experience for the evaluation of runway capacity at general aviation airports, most of these studies are aimed at civil airports. Civil airports have large-scale runways, complex operational methods, and relatively difficult runway capacity assessments. Therefore, these studies often focus on a specific aspect of the runway capacity assessment system and less on the overall opera-

tional perspective. General aviation airports are small in scale and have simple operating methods; a systematic assessment of their runway capacity is needed to reflect the objective reality of general aviation airports. Moreover, civil airports mostly operate under radar control, where aircraft can enter the arrival procedure as long as safety is ensured, but general aviation airports mostly operate under procedural control, where only one aircraft is typically allowed in the same spatial area at a time. This results in the aircraft not only occupying a runway during the arrival process but also occupying part of the air space during departure and arrival. Therefore, it is not feasible to apply the aforementioned results directly to the runway capacity assessment of general aviation airports. It is necessary to combine the actual operation of general aviation airports and construct a systematic and comprehensive evaluation model to obtain reasonable assessment results.

Based on this, this paper proposes a method for assessing the runway capacity of general aviation airports based on the runway expansion system, aiming to explore the universal methods applicable to the runway capacity assessment of general aviation airports from both theoretical and engineering perspectives. Specifically, it primarily focuses on the concept of the runway expansion system, conducting innovative construction and exploration of the evaluation model, and demonstrates the feasibility and rationality of the proposed evaluation model through designed experiments. The specific content is arranged as follows. First, it introduces the flight rules of general aviation airports and the departure and arrival procedures with symmetrical characteristics, such as a left/right traffic pattern and left/right racetrack, to understand the basic operational patterns and flight characteristics of general aviation airports. Second, in light of the flight characteristics of general aviation, fully considering the mutually exclusive nature of aircraft using the runway, a runway extension system is constructed for the symmetrical activities of aircraft departure and arrival, covering both the visual flight rule (VFR) and instrument flight rule (IFR). Third, based on the proposed runway extension system, runway capacity assessment models are established for general aviation airports under arrival, departure, and mixed operation modes. Fourth, a case study is conducted on a certain general aviation airport in China, and three sets of numerical experiments are designed to analyze the impact of parameters with certain symmetrical relationships, such as flight rule, flight procedure, and flight intervals, on runway capacity and to verify the rationality of the established models, with the aim of providing a reference for strengthening the construction of general aviation airports.

2. General Aviation Airport Flight Rules and Procedures

2.1. General Aviation Airport Flight Rules

General aviation airports usually provide procedural control services for aircraft. ATCs need to configure the appropriate safety spacing between aircraft based on the position information reported by pilots, in accordance with the relevant flight rules. Depending on the meteorological conditions, the flight rule in procedural control can be divided into the VFR and IFR, with the corresponding flight activities being visual flight and instrument flight. Visual flight [30] refers to flight where the aircraft's flight status and orientation are determined by visual means under conditions of a visible horizon and landmarks. Instrument flight [31] refers to flight where the pilot determines the aircraft's flight status and position entirely or partially by using the aircraft's instruments.

2.2. General Aviation Airport Visual Flight Procedure

2.2.1. Traffic Pattern

The traffic pattern is a procedure established around the airport runway for aircraft takeoff and landing [32]. Under the VFR, aircraft typically follow the traffic pattern for arrivals and departures. The traffic pattern is roughly rectangular in shape, consisting of five legs, and can be divided into left and right traffic patterns, as shown in Figure 1.

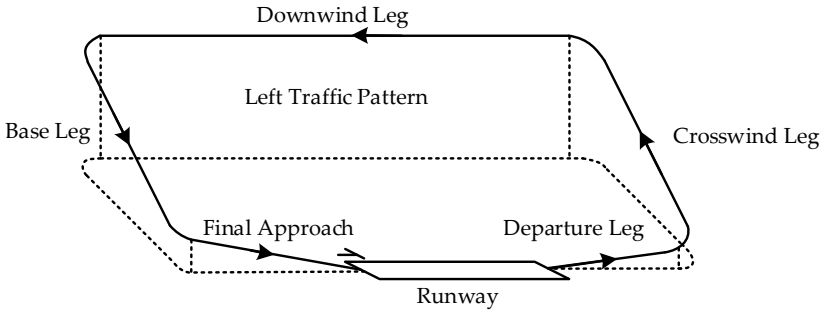

Figure 1. Left traffic pattern.

When the aircraft arrives, it can sequentially join the various legs and turning points of the traffic pattern for landing. When the aircraft departs, in addition to departing directly, the ATC may instruct the aircraft to establish a left or right traffic pattern for turning departure after takeoff.

2.2.2. Short Approach

Under normal circumstances, the flight time of an aircraft in the traffic pattern is relatively long. To accelerate the arrival and departure process, some general aviation airports have established a short approach for aircraft to use for takeoff and landing [33]. The shape of the short approach is similar to the traffic pattern, but it is narrower and at a lower altitude. Once an aircraft joins the short approach, it can maintain a descending attitude throughout, shorten the flight distance, and achieve a quick landing, as shown in Figure 2.

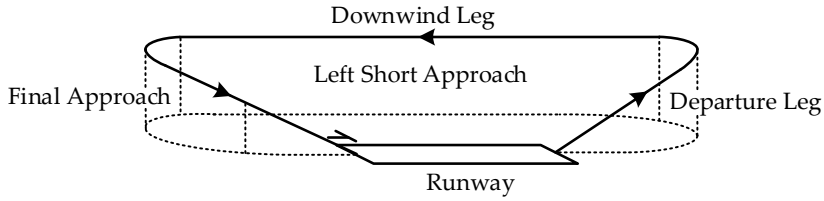

Figure 2. Left short approach.

When the aircraft arrives, it establishes a short approach along the direction of landing through the airport for landing. When the aircraft departs, in addition to departing directly, the ATC may instruct the aircraft to establish a left or right short approach for turning departure after takeoff.

2.3. General Aviation Airport Instrument Flight Procedure

2.3.1. Teardrop Pattern Procedure

The teardrop pattern procedure [34] uses the airport radio station or navigation aid as the initial approach fix (IAF), where the arriving aircraft passes through this point and maintains a certain rate of descent for a period of time before turning to intercept the intermediate approach fix (IF) or final approach fix (FAF), before landing towards the runway. This is shown in Figure 3.

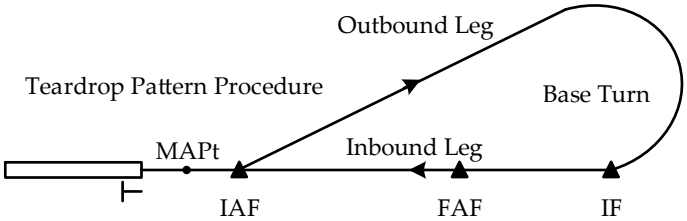

Figure 3. Teardrop pattern procedure.

When the aircraft arrives, it directly joins the teardrop pattern procedure for landing by passing through the FAF. When the aircraft departs, in addition to direct departure, the ATC may instruct the aircraft to make a left or right turn after takeoff and pass through the FAF to establish the teardrop pattern procedure for departure.

2.3.2. Racetrack

The racetrack [35] uses the airport radio station or navigation aid as the IAF. Arriving aircraft maintain the prescribed course towards the landing direction through this point, make a 180° turn to the left or right, fly along the third leg for the specified time, descend to the specified altitude, continue in the same direction to make another 180° turn, and subsequently land towards the runway. This is shown in Figure 4.

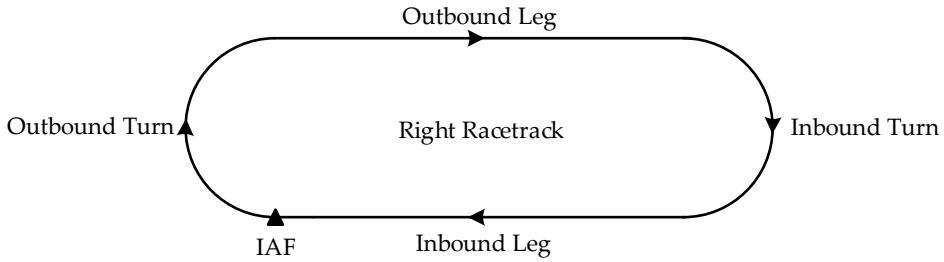

Figure 4. Right racetrack.

When the aircraft arrives, it should pass over the station along the landing heading and then join the racetrack for landing. When the aircraft departs, in addition to direct departure, the ATC may instruct the aircraft to make a turn over the navigation aid after takeoff to join the racetrack.

3. General Aviation Airport Runway Extension System

3.1. Visual Flight Rule Runway Extension System

Under the VFR, for two aircraft using the traffic pattern to land, the second aircraft is only allowed to enter the final approach after the preceding aircraft has touched down. For two aircraft taking off, the second aircraft may only be permitted to take off after the preceding aircraft has entered the crosswind leg or has reached a distance of 100 m during the day or 150 m at night after becoming airborne. For landing and taking off, if there is an aircraft on final approach for the landing of the traffic pattern, the aircraft taking off is not allowed to enter the runway. It is evident that there is an exclusionary characteristic during the aircraft's use of the runway, primarily manifested in the runway system that has been expanded in time and space based on flight safety separation criteria. Based on these characteristics, the concept of a Visual Flight Rule Runway Extension System (VFR-RES) is proposed here, as shown in Figure 5.

The VFR-RES is represented by the short dashed line in Figure 5a. It starts from the entry point of the traffic pattern's final approach as the RES entrance and ends at the starting position of the traffic pattern's crosswind leg or the area where the flight altitude reaches 100 m during the day and 150 m at night as the RES exit. It includes the airspace and ground areas of the traffic pattern's departure leg, final approach, short approach, and runway. Figure 5b depicts the VFR-RES during landing, with the starting position of the traffic pattern's final approach as the RES entrance and the exit taxiway used by the aircraft to leave the runway as the RES exit. Figure 5c depicts the VFR-RES during takeoff, with the takeoff end of the runway as the RES entrance and the starting position of the traffic pattern's crosswind leg, the completion position of the first turn in the short approach, or the area where the flight altitude reaches 100 m during the day and 150 m at night as the RES exit. To avoid flight conflicts, control points should be established on the downwind leg of the traffic pattern and the public approach lane. Once an aircraft on the traffic pattern enters a control point, any aircraft on the public approach lane must maintain

the prescribed safety separation before reaching the control point, and the same applies in the opposite direction.

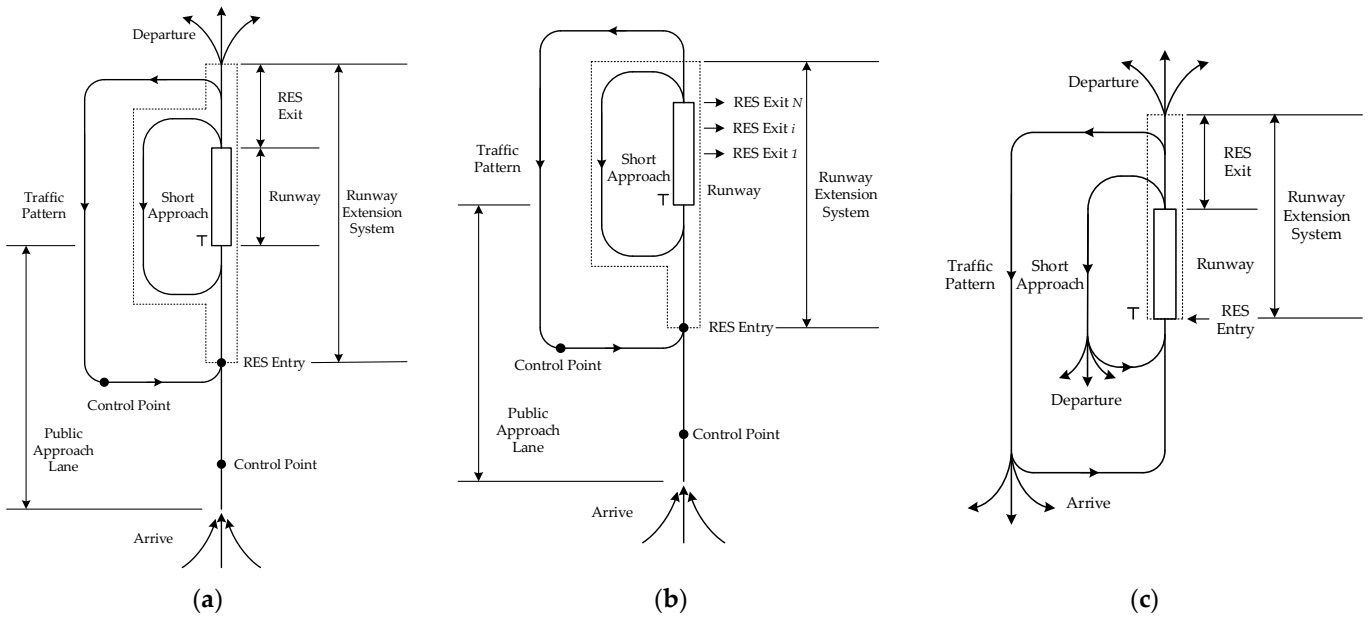

Figure 5. Visual flight rule runway extension system. (**a**) Overall schematic diagram; (**b**) Landing scenario schematic diagram; (**c**) Takeoff scenario schematic diagram.

3.2. Instrument Flight Rule Runway Extension System

Under the IFR, for two aircraft using the same approach procedure for landing, the second aircraft is allowed to enter the inbound leg only after the preceding aircraft is about to leave the runway. For two aircraft taking off, the second aircraft is permitted to take off only after the leading aircraft has departed and the vortex separation standards are met. For landing and taking off aircraft, when there is an aircraft on final approach for landing on the inbound leg, the aircraft taking off is not allowed to enter the runway. It is evident that aircraft under the Instrument Flight Rule also exhibit mutually exclusive characteristics during the runway usage process. Based on these characteristics, the concept of an Instrument Flight Rule Runway Extension System (IFR-RES) is proposed here, as shown in Figures 6 and 7.

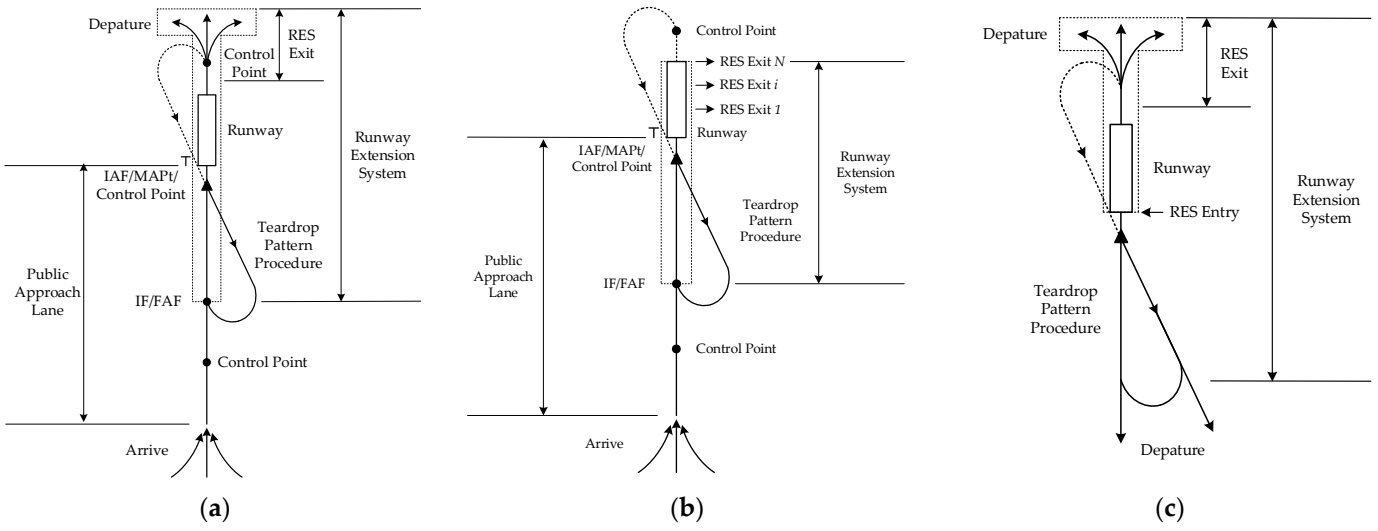

Figure 6. Instrument flight rule runway extension system (Teardrop Pattern Procedure). (**a**) Overall schematic diagram; (**b**) Landing scenario schematic diagram; (**c**) Takeoff scenario schematic diagram.

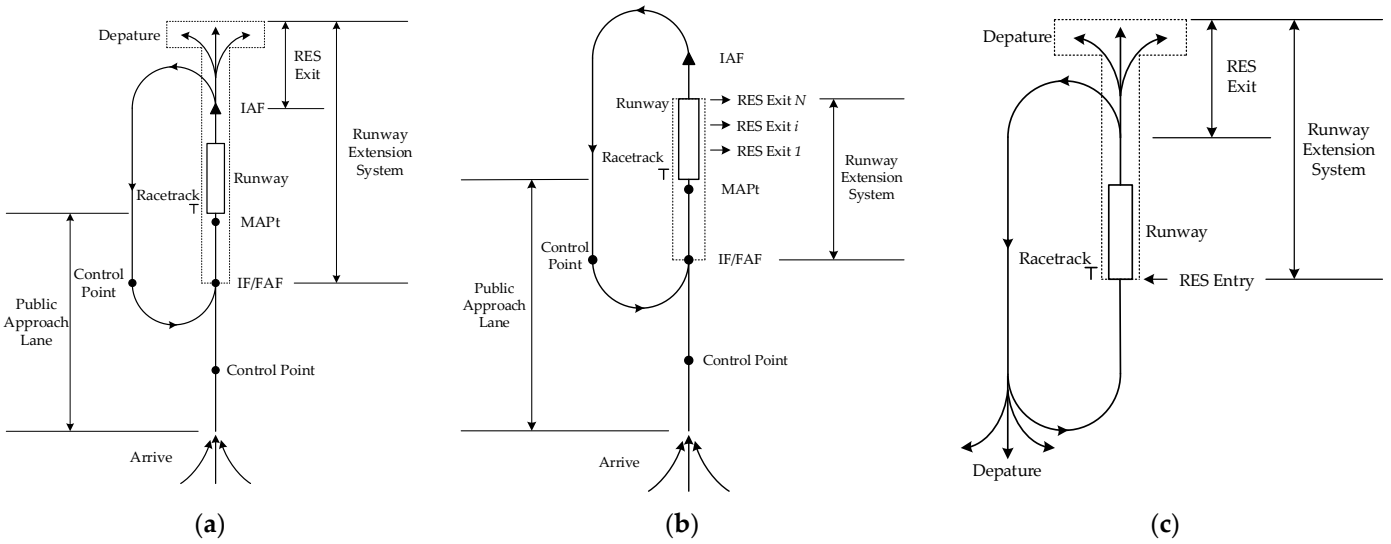

Figure 7. Instrument flight rule runway extension system (Racetrack). (**a**) Overall schematic diagram; (**b**) Landing scenario schematic diagram; (**c**) Takeoff scenario schematic diagram.

Figures 6a and 7a show the IFR-RES for the two procedures with short dashed lines. Both use the IF or FAF as the RES entry point and the sectors of the direct or left/right turn departure leg that meet the takeoff safety separation criteria as the RES exit. Figures 6b and 7b depict the IFR-RES for the two procedures during landing, with the IF or FAF point as the RES entry and the taxiway used by the aircraft to exit the runway as the RES exit. Figures 6c and 7c depict the IFR-RES for the two procedures during takeoff, with the runway takeoff end as the RES entry and the sectors of the direct or left/right turn departure leg that meet the takeoff safety separation criteria as the RES exit. To avoid flight conflicts between aircraft approaching from different directions, control points should be set at the starting position of the left turn over the navigation aid in the teardrop pattern procedure and at the public approach lane, as well as at the starting position of the inbound leg of the racetrack and at the public approach lane, to ensure that aircraft maintain the prescribed safety separation.

4. Model for Evaluating the Runway Capacity of General Aviation Airports Based on the Runway Extension System

4.1. Capacity of Runway Extension System

Definition 1. *The capacity of the RES represents the maximum number of aircraft movements that the RES can serve per unit of time. It is generally expressed as the weighted average of the service time for all types of aircraft by the RES, as shown in Formulas (1) and (2).*

$$C_{VFR/IFR} = \frac{1}{E[T]}, \tag{1}$$

$$E[T] = \sum_{i=1}^{n} \sum_{j=1}^{n} p_{ij} T_{ij}, \tag{2}$$

Wherein, $C_{VFR/IFR}$ represents the capacity of the VFR-RES or IFR-RES, its unit is sorties per hour; $E[T]$ represents the average service time of the runway extension system capacity, its unit is hour; p_{ij} represents the probability that the preceding aircraft is type i and the following aircraft is type j; and T_{ij} represents the time separation between aircraft i and aircraft j, its unit is hour. However, to align with the actual work of the ATC, the unit should be minutes or seconds during the calculation process, and it needs to be converted back to hours when calculating the final capacity. For the sake of convenience in calculation, the units used in this text are seconds.

In actual flight operations, aircraft arrive from different directions. Regardless of the landing method used by the aircraft, in the subsequent modeling process, it can be understood that the aircraft are landing on a public approach lane. The following analysis is conducted with reference to Figure 8.

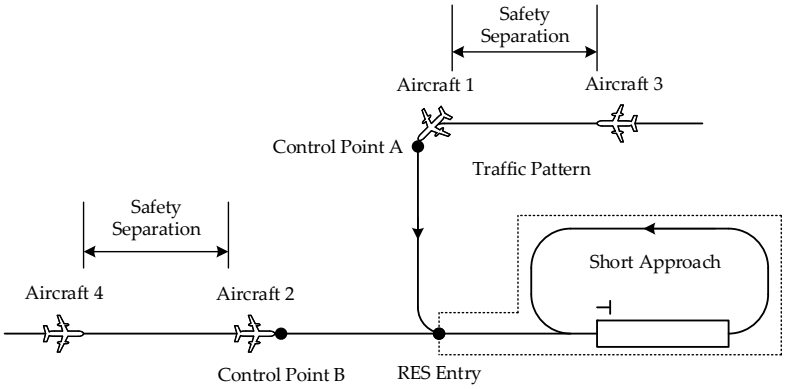

Figure 8. Visual flight rule aircraft landing situation diagram.

When aircraft 1 and aircraft 4 land using the traffic pattern and short approach, respectively, aircraft 4 must maintain a safety separation from control point B when aircraft 1 reaches control point A. Since the distance from control points A and B to the RES entry is the same, it is evident that aircraft 1 and aircraft 4 can be understood as both landing on the common landing approach path. The same applies to aircraft 2 and aircraft 3.

4.2. General Aviation Airport Single Runway Arrival Capacity Evaluation Model

4.2.1. General Aviation Airport Single Runway Arrival Capacity Analysis

As indicated by Formula (2), the arrival capacity of a single runway at a general aviation airport is primarily determined by the combination probability of landing aircraft and the time separation between them. To ensure flight safety, during the aerial approach phase, the actual time separation between aircraft must not be less than the prescribed time separation for successive arriving aircraft. When entering the RES for landing, the actual time separation between aircraft must not be less than the prescribed occupancy time of the RES for successive arriving aircraft. The time separation between aircraft should be configured according to the maximum value of the aforementioned time separation regulations. Therefore, the expression for the time separation between successive arriving aircraft is as shown in Formula (3).

$$T_{ij}(AA) = \max(ARORES(i) \quad AASRES(ij)), \tag{3}$$

Wherein, $T_{ij}(AA)$ represents the time separation between successive arriving aircraft; $ARORES(i)$ represents the time regulation for the occupancy of the RES by successive arriving aircraft; and $AASRES(ij)$ represents the time separation regulation between successive arriving aircraft. The units of the aforementioned functions should be in seconds.

4.2.2. Successive Arriving Aircraft Runway Extension System Occupancy Time Regulation

Assuming that $AASRES(ij)$ is not taken into account, the time separation between successive arriving aircraft must meet the requirement $T_{ij}(AA) \geq ARORES(i)$. Based on this, the derivation of the formula for $ARORES(i)$ is presented below.

$ARORES(i)$ is primarily determined by the RES occupancy time $ARES_i$ of the preceding aircraft, which is composed of the flight time from when aircraft i enters the runway extension system until it reaches the runway end, as well as the runway occupancy time. This is shown in Formula (4).

$$ARORES(i) = ARES_i = t_{RESi} + AR_i, \tag{4}$$

Wherein, $ARES_i$ represents the RES occupancy time for aircraft i; t_{RESi} represents the flight time from when aircraft i enters the RES until it reaches the runway; and AR_i represents the runway occupancy time for aircraft i. The units of the aforementioned functions should be in seconds.

(1) Runway occupancy time

AR_i consists of the aircraft's landing deceleration time, taxiing time, and taxiway occupancy time. Among these, the taxiing time and exit runway time are mainly related to the position where the aircraft exits the runway and the type of taxiway used, as shown in Figure 9.

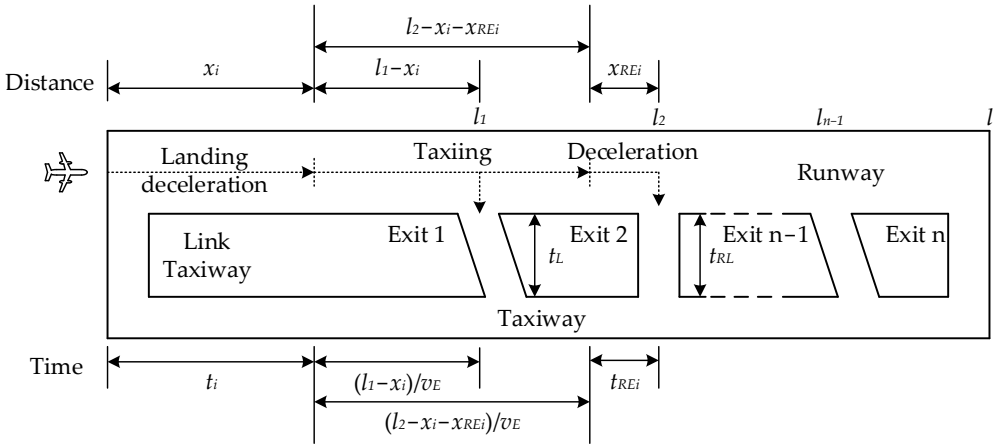

Figure 9. Schematic diagram of a general aviation airport runway configuration.

As illustrated, Exit 1 and Exit $n-1$ are rapid link taxiways, while Exit 2 and Exit n are common link taxiways. When an aircraft enters a rapid link taxiway, it maintains its taxiing speed. When an aircraft enters a common link taxiway, it should reduce its taxiing speed to the safety standard before proceeding to depart via the common link taxiway. The expression for the runway occupancy time AR_i of aircraft i is shown in Formula (5).

$$AR_i = \begin{cases} t_i + \frac{l_n - x_i}{v_E} + t_L, & \text{Exit n is the rapid link taxiway} \\ t_i + \frac{l_n - x_i - x_{REi}}{v_E} + t_{REi} + t_{RL}, & \text{Exit n is the common link taxiway} \end{cases}, \quad (5)$$

Wherein, x_i and t_i represent the distance and time, respectively, that the aircraft takes to decelerate from touch-down to the disengagement speed v_E, their units are meters, seconds, and meters per second, respectively; x_{REi} and t_{REi} represent the distance and time, respectively, that the aircraft takes to decelerate from the disengagement speed to a speed safe enough to enter the regular taxiway, their units are meters and seconds, respectively; t_L and t_{RL} represent the time the aircraft occupies on the express taxiway and the regular taxiway, respectively, their units are seconds; and l_n indicates the distance from the runway entrance to the exit n, its unit is meters.

(2) Visual Flight Rule Successive Arriving Aircraft Runway Extension System Occupancy Time Regulations

The occupancy time of the RES for successive arriving aircraft under the VFR is mainly affected by factors such as the flight time on the final approach, the flight time on short approach, and the runway occupancy time. Then, the expression for $ARES_i$ is as shown in Formula (6).

$$ARES_i = \begin{cases} t_{FAi} + AR_i, & \text{i is for the aircraft joining the traffic pattern} \\ t_{SAi} + AR_i, & \text{i is for the aircraft joining the short approach} \end{cases}, \quad (6)$$

Wherein, t_{FAi} represents the flight time of the aircraft from the final approach to the runway end and t_{SAi} represents the flight time of the aircraft from joining the short approach to the runway end. The units of the aforementioned functions should be in seconds.

Suppose there are l landing aircraft, with l_1 aircraft using the short traffic pattern for landing and $l - l_1$ aircraft using the standard traffic pattern for landing. The landing airport has a total of m rapid link taxiways and n common link taxiways. The expression for the average occupancy time of the RES for aircraft i is shown in Formula (7).

$$E(ARES_i) = \begin{cases} t_{NPi} + P(i_{RLT}) \sum\limits_{i_m=1}^{m} P(i_m)\left(t_i + \dfrac{l_n - x_i}{v_E} + t_L\right) + P(i_{CLT}) \sum\limits_{i_n=1}^{n} P(i_n)\left(t_i + \dfrac{l_n - x_i - x_{REi}}{v_E} + t_{REi} + t_{RL}\right), & 1 \le i \le l_1 \\ t_{SAi} + P(i_{RLT}) \sum\limits_{i_m=1}^{m} P(i_m)\left(t_i + \dfrac{l_n - x_i}{v_E} + t_L\right) + P(i_{CLT}) \sum\limits_{i_n=1}^{n} P(i_n)\left(t_i + \dfrac{l_n - x_i - x_{REi}}{v_E} + t_{REi} + t_{RL}\right), & l_1 + 1 \le i \le l \end{cases}, \quad (7)$$

Wherein, $P(i_{RLT})$ and $P(i_{CLT})$ represent the probability of an aircraft choosing to exit the runway via the rapid link taxiway and the common link taxiway, respectively; $P(i_m)$ and $P(i_n)$ represent the probability of an aircraft exiting the runway from the m rapid link taxiway and the n common link taxiway, respectively; $P(i_{RLT}) + P(i_{CLT}) = 1$; $\sum\limits_{i_m=1}^{m} P(i_m) = 1$; $\sum\limits_{i_n=1}^{n} P(i_n) = 1$.

Let $ARES_i$ and $T_{ij}(AA)$ in the VFR be independent of each other, and $ARES_i \sim N\left(\overline{ARES_i}, \sigma_{ARES}^2\right)$, $T_{ij}(AA) \sim N\left(ARORES(i), \sigma_0^2\right)$. Let the random errors in flight be e_0, $e_0 \sim N\left(0, \sigma_0^2\right)$. The standard normal distribution Z can be obtained, as shown in Formula (8).

$$Z = \frac{\left(T_{ij}(AA) - ARES_i\right) - \left(ARORES(i) - \overline{ARES_i}\right)}{\sqrt{\sigma_0^2 + \sigma_{ARES}^2}} \sim N(0,1), \quad (8)$$

When $T_{ij}(AA) < ARORES(i)$ occurs, the flight safety separation regulations are violated. Let the probability of violating the flight safety separation regulations be p_v. The expression for p_v can be obtained, as shown in Formula (9).

$$\begin{aligned} & p_v \\ & = P\left[T_{ij}(AA) < ARES_i\right] \\ & = P\left[\frac{\left(T_{ij}(AA) - ARES_i\right) - \left(ARORES(i) - \overline{ARES_i}\right)}{\sqrt{\sigma_0^2 + \sigma_{ARES}^2}} < -\frac{\left(ARORES(i) - \overline{ARES_i}\right)}{\sqrt{\sigma_0^2 + \sigma_{ARES}^2}}\right] \end{aligned}, \quad (9)$$

Let:

$$Z_1 = -\frac{\left(ARORES(i) - \overline{ARES_i}\right)}{\sqrt{\sigma_0^2 + \sigma_{ARES}^2}}, \quad (10)$$

Since $Z \sim N(0,1)$, according to the properties of the normal distribution, let the probability that successive arriving aircraft meet the flight safety separation regulations be p_c. The expression for p_c can be obtained, as shown in Formula (11).

$$p_c = 1 - P[Z < -Z_1] = P\left[Z < -\frac{\left(ARORES(i) - \overline{ARES_i}\right)}{\sqrt{\sigma_0^2 + \sigma_{ARES}^2}}\right] = \Phi(Z_1), \quad (11)$$

Thus, the expression for the inverse function of $\Phi(Z_1)$ can be obtained, and accordingly, the expression for VFR successive arriving aircraft RES occupancy time regulations is as shown in Formula (12).

$$ARORES(i) = \overline{ARES_i} + \Phi^{-1}(p_c)\sqrt{\sigma_0^2 + \sigma_{ARES}^2}, \quad (12)$$

Wherein, the unit of $ARORES(i)$ is seconds.

(3) Instrument Flight Rule Successive Arriving Aircraft Runway Extension System Occupancy Time Regulations

The occupancy time of the RES for successive arriving aircraft under the IFR is mainly affected by factors such as the flight time on the inbound leg in the two procedures, as well as the runway occupancy time. Then, the expression for $ARES_i$ is as shown in Formula (13).

$$ARES_i = \begin{cases} t_{TPi} + AR_i, & \text{i is for the aircraft joining the teardrop pattern procedure} \\ t_{RTi} + AR_i, & \text{i is for the aircraft joining the racetrack} \end{cases}, \quad (13)$$

Wherein, t_{TPi} and t_{RTi} represent the flight time from when the aircraft enters the inbound leg of the two procedures until it reaches the runway end, respectively. The units of the aforementioned functions should be in seconds.

Suppose there are l landing aircraft, with the l_1 aircraft using the teardrop pattern procedure for landing and the $l - l_1$ aircraft using the racetrack for landing. The landing airport has a total of m rapid link taxiways and n common link taxiways. The expression for the average occupancy time of the RES for aircraft i is shown in Formula (14).

$$E(ARES_i) = \begin{cases} t_{TPi} + P(i_{RLT}) \sum\limits_{i_m=1}^{m} P(i_m) \left(t_i + \dfrac{l_n - x_i}{v_E} + t_L \right) + P(i_{CLT}) \sum\limits_{i_n=1}^{n} P(i_n) \left(t_i + \dfrac{l_n - x_i - x_{REi}}{v_E} + t_{REi} + t_{RL} \right), & 1 \le i \le l_1 \\ t_{RTi} + P(i_{RLT}) \sum\limits_{i_m=1}^{m} P(i_m) \left(t_i + \dfrac{l_n - x_i}{v_E} + t_L \right) + P(i_{CLT}) \sum\limits_{i_n=1}^{n} P(i_n) \left(t_i + \dfrac{l_n - x_i - x_{REi}}{v_E} + t_{REi} + t_{RL} \right), & l_1 + 1 \le i \le l \end{cases}, \quad (14)$$

Let $ARES_i$ and $T_{ij}(AA)$ in the IFR be independent of each other, and $ARES_i \sim N\left(\overline{ARES_i}, \sigma^2_{ARES}\right)$, $T_{ij}(AA) \sim N\left(ARORES(i), \sigma_0^2\right)$. Let the random errors in flight be e_0, $e_0 \sim N\left(0, \sigma_0^2\right)$. Let the probability that successive arriving aircraft meet the flight safety separation regulations be p_c. In a simplified calculation process, the expression for IFR successive arriving aircraft RES occupancy time regulations is as shown in Formula (15).

$$ARORES(i) = \overline{ARES_i} + \Phi^{-1}(p_c)\sqrt{\sigma_0^2 + \sigma^2_{ARES}}, \quad (15)$$

Wherein, the unit of $ARORES(i)$ is seconds.

4.2.3. Successive Arriving Aircraft Time Separation Regulation

Assuming that $ARORES(i)$ is not taken into account, the time separation between successive arriving aircraft must meet the requirement $T_{ij}(AA) \ge AASRES(i)$. Based on this, the derivation of the formula for $AASRES(i)$ is presented below.

Let the time separation $T_{ij}(AA)$ between successive arriving aircraft be a random variable, and $T_{ij}(AA) \sim N\left(\overline{T_{ij}(AA)}, \sigma_0^2\right)$. In the absence of random errors, the expression for $AASRES(i)$ can be obtained, as shown in Equation (16).

$$AASRES(ij) = \overline{T_{ij}(AA)}, \quad (16)$$

Wherein, all functions are in units of seconds.

Let the buffer time be B_{ij} and let the arrival separation be M_{ij} as specified in the relevant flight rule. The expression for $T_{ij}(AA)$ and $\overline{T_{ij}(AA)}$ can be obtained, as shown in Equations (17) and (18).

$$T_{ij}(AA) = M_{ij} + B_{ij} + e_0, \quad (17)$$

$$\overline{T_{ij}(AA)} = M_{ij} + B_{ij}, \quad (18)$$

Wherein, the unit for all functions, except for the random variable e_0, is seconds.

(1) Visual Flight Rule Successive Arriving Aircraft Time Separation Regulation

The flight safety separation under the VFR is mainly controlled by the pilot's own judgment; therefore, the minimum separation between two aircraft should be achieved at the entrance of the RES and is unrelated to the flight distance during the landing process.

Let the minimum separation distance δ_{ij} be the distance reached at the entrance of the extended runway system by successive arriving aircraft, and the flying speed of the following aircraft j is V_j. Then, the expression for M_{ij} can be obtained, as shown in Formula (19).

$$M_{ij} = \frac{\delta_{ij}}{v_j}, \tag{19}$$

Wherein, the unit of δ_{ij} is meters, the unit of v_j is meters per second, and the unit of M_{ij} is seconds.

When $T_{ij}(AA) < M_{ij}$ occurs, the flight safety separation regulations are violated. Let the probability that successive arriving aircraft meet the flight safety separation regulations be p_c. In a simplified calculation process, the expression for the buffer time B_{ij} can be obtained, as shown in Formula (20).

$$B_{ij} = \sigma_0 \Phi^{-1}(p_c), \tag{20}$$

Wherein, the unit of B_{ij} is seconds.

The expression for VFR successive arriving aircraft time separation regulations is as shown in Formula (21).

$$AASRES(ij) = \overline{T_{ij}(AA)} = \frac{\delta_{ij}}{v_j} + \sigma_0 \Phi^{-1}(p_c), \tag{21}$$

Wherein, the unit of $AASRES(ij)$ is seconds.

(2) Instrument Flight Rule Successive Arriving Aircraft Time Separation Regulation

The flight safety separation under the IFR is mainly arranged by the ATC in accordance with regulations. In the IFR, depending on the flight speed, successive arriving aircraft can be divided into two situations: approaching and receding, as shown in Figure 10.

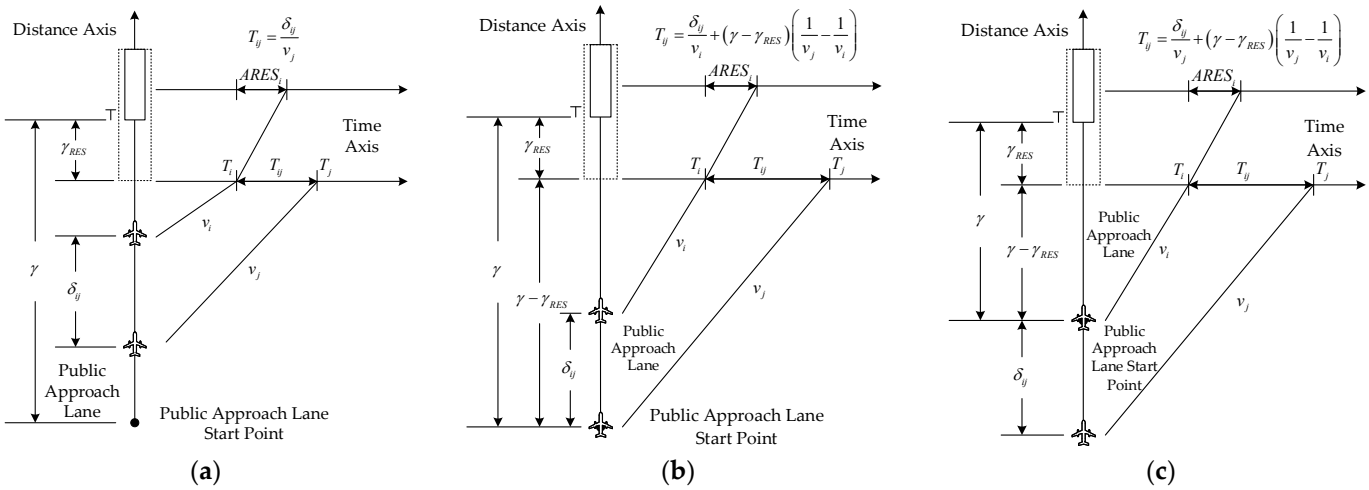

Figure 10. Successive arriving aircraft posture diagram. (**a**) Approaching situation; (**b**) Receding situation (Minimum separation inside); (**c**) Receding situation (Minimum separation outside).

Let $(*)$ and $(**)$ represent the minimum separation under the condition of a receding situation, inside and outside the starting point of the public approach lane, respectively. It is important to note that under the receding situation, $T_{ij}(*) < T_{ij}(**)$, $T_{ij}(*)$ can be regarded as the strict minimum separation between successive arriving aircraft in the receding situation. That is, when the preceding aircraft reaches a point where the distance is δ_{ij} within the starting point of the public approach lane, the following aircraft must not enter the starting point of the public approach lane, otherwise it will violate the flight

safety separation regulations. Consequently, the expression for M_{ij} in $T_{ij}(AA)$ under the condition of a receding situation can be derived, as shown in Equation (22).

$$M_{ij} = T_j - T_i = \frac{(\gamma - \gamma_{RES}) + \delta_{ij}}{v_j} - \frac{(\gamma - \gamma_{RES})}{v_i} = \frac{\delta_{ij}}{v_j} + (\gamma - \gamma_{RES})\left(\frac{1}{v_j} - \frac{1}{v_i}\right), \quad (22)$$

Wherein, γ represents the length of the common landing route, its unit is meters; γ_{RES} represents the length of the route included in the RES, its unit is meters; δ_{ij} represents the minimum safe separation distance, its unit is meters; v_i represents the speed of aircraft i, its unit is meters per second; and v_j represents the speed of aircraft j, its unit is meters per second.

When $T_{ij}(AA) < M_{ij}$ occurs, the flight safety separation regulations are violated. Let the probability that successive arriving aircraft meet the flight safety separation regulations be p_c. In a simplified calculation process, the expression for the buffer time B_{ij} can be obtained, as shown in Formula (23).

$$B_{ij} = \begin{cases} \sigma_0 \Phi^{-1}(p_c), & v_i \le v_j \\ \sigma_0 \Phi^{-1}(p_c) - \delta_{ij}\left(\frac{1}{v_j} - \frac{1}{v_i}\right), & v_i > v_j \end{cases}, \quad (23)$$

Wherein, the unit of B_{ij} is seconds.

The expression for IFR successive arriving aircraft time separation regulations is as shown in Formula (24).

$$AASRES(ij) = \overline{T_{ij}(AA)} = \begin{cases} \frac{\delta_{ij}}{v_j} + \sigma_0 \Phi^{-1}(p_c), & v_i \le v_j \\ \delta_{ij}\left(\frac{2}{v_i} - \frac{1}{v_j}\right) + (\gamma - \gamma_{RES})\left(\frac{1}{v_j} - \frac{1}{v_i}\right) + \sigma_0 \Phi^{-1}(p_c), & v_i > v_j \end{cases}, \quad (24)$$

Wherein, the unit of $AASRES(ij)$ is seconds.

4.2.4. General Aviation Airport Single Runway Arrival Capacity

According to Formulas (1) and (2), and the derivation results from Sections 4.2.2 and 4.2.3, the expression for the single runway arrival capacity of general aviation airports under the VFR and IFR can be obtained, as shown in Formula (25).

$$C_{VFR/IFR}(AA) = \frac{1}{\sum_{i=1}^{n}\sum_{j=1}^{n} p_{ij}\left[\max\left(ARORES(i)_{VFR/IFR} \quad AASRES(ij)_{VFR/IFR}\right)\right]}, \quad (25)$$

Wherein, $C_{VFR/IFR}(AA)$ represents the single runway arrival capacity under the VFR or IFR, its unit is sorties per hour; p_{ij} represents the probability that the preceding aircraft is type i and the following aircraft is type j; $p_{ij} = p_i \cdot p_j$, $p_{ij} > 0$, $\sum_{i=1}^{n}\sum_{j=1}^{n} p_{ij} = 1$.

To ensure flight safety, during actual flight operations, when transitioning from the VFR to the IFR or from the IFR to the VFR, the appropriate safety separation should be configured between successive aircraft according to the IFR. Therefore, the expression for the single runway arrival capacity of general aviation airports can be obtained, as shown in Formula (26).

$$C(AA) = \sum_{i=1}^{n}\sum_{j=1}^{n} p_{ij_{VFR}} C_{VFR}(AA) + \left(1 - \sum_{i=1}^{n}\sum_{j=1}^{n} p_{ij_{VFR}}\right) C_{IFR}(AA), \quad (26)$$

Wherein, $C(AA)$ represents the single runway arrival capacity of a general aviation airport, its unit is sorties per hour; $p_{ij_{VFR}}$ represents the proportion that successive arriving aircraft i and j both land according to the VFR.

4.3. General Aviation Airport Single Runway Departure Capacity Evaluation Model

4.3.1. General Aviation Airport Single Runway Departure Capacity Analysis

Similar to Section 4.2.1, the time separation in the departure capacity of a single runway at general aviation airports is mainly affected by the regulations on the occupation time of the RES for successive departing aircraft and the regulations on the time separation between successive departing aircraft. Therefore, the actual time separation between aircraft should be configured according to the maximum value of the aforementioned two time separation regulations. As introduced in Sections 2.2 and 2.3, the departure procedures for the VFR and IFR are essentially the same. Therefore, a unified derivation of the single runway departure capacity evaluation model for general aviation airports under the VFR and IFR is provided here. Therefore, the expression for the time separation between successive departing aircraft is shown in Equation (27).

$$T_{ij}(DD) = \max\left(DRORES(i) \quad DDSRES(ij)\right), \tag{27}$$

Wherein, $T_{ij}(DD)$ represents the time separation between successive departing aircraft; $DRORES(i)$ represents the time regulation for the occupancy of the RES by successive departing aircraft; and $DDSRES(ij)$ represents the time separation regulation between successive departing aircraft. The units of the aforementioned functions should be in seconds.

4.3.2. Successive Departing Aircraft Runway Extension System Occupancy Time Regulation

Assuming that $DDSRES(ij)$ is not taken into account, the time separation between successive departing aircraft must meet the requirement $T_{ij}(DD) \geq DRORES(i)$. Based on this, the derivation of the formula for $DRORES(i)$ is presented below.

$DRORES(i)$ is primarily determined by the RES occupancy time $DRES_i$ of the preceding aircraft, which is composed of the runway occupancy time and the flight time from the aircraft leaving the runway until it reaches the exit of the RES. This is shown in Formula (28).

$$DRORES(i) = DRES_i = DR_i + t_{RESi}, \tag{28}$$

Wherein, $DRES_i$ represents the RES occupancy time for aircraft i; AR_i represents the runway occupancy time for aircraft i; and t_{RESi} represents the flight time from aircraft i leaving the runway until it reaches the exit of the RES. The units of the aforementioned functions should be in seconds.

The occupancy time of the RES for successive departing aircraft is mainly affected by factors such as the flight time of the aircraft during direct departure or turning departure, and runway occupancy time. Then, the expression for $DRES_i$ is as shown in Formula (29).

$$DRES_i = \begin{cases} DR_i + t_{DDi}, & \text{i is for the aircraft that the departs directly} \\ DR_i + t_{TDi}, & \text{i is for the aircraft that the departs with a turn} \end{cases}, \tag{29}$$

Wherein, t_{DDi} represents the flight time of an aircraft when it departs directly from the RES and t_{TDi} represents the flight time of an aircraft when it departs with a turn from the RES. The units of the aforementioned functions should be in seconds.

Correspondingly, the expression for the average occupancy time of the RES for aircraft i is shown in Formula (30).

$$E(DRES_i) = DR_i + p_{DDi}t_{DDi} + p_{TDi}t_{TDi}, \tag{30}$$

Wherein, p_{DDi} represents the probability of an aircraft taking off directly; p_{TDi} represents the probability of an aircraft taking off after making a turn; $p_{DDi} + p_{TDi} = 1$.

Let $DRES_i$ and $T_{ij}(DD)$ be independent of each other, and $DRES_i \sim N\left(\overline{DRES_i}, \sigma^2_{DRES}\right)$, $T_{ij}(DD) \sim N\left(DRORES(i), \sigma_0^2\right)$. Let the random errors in flight be e_0, $e_0 \sim N\left(0, \sigma_0^2\right)$. Let the probability that successive departing aircraft meet the flight safety separation regu-

lations be p_c. In a simplified calculation process, the expression for successive departing aircraft RES occupancy time regulations is as shown in Formula (31).

$$DRORES(i) = \overline{DRES}_i + \Phi^{-1}(p_c)\sqrt{\sigma_0^2 + \sigma_{DRES}^2}, \tag{31}$$

Wherein, the unit of $DRORES(i)$ is seconds.

4.3.3. Successive Departing Aircraft Time Separation Regulation

Assuming that $DRORES(i)$ is not taken into account, the time separation between successive departing aircraft must meet the requirement $T_{ij}(DD) \geq DDSRES(i)$. Based on this, the derivation of the formula for $DDSRES(i)$ is presented below.

Let the time separation $T_{ij}(DD)$ between successive departing aircraft be a random variable, and $T_{ij}(DD) \sim N\left(\overline{T_{ij}(DD)}, \sigma_0^2\right)$. In the absence of random errors, the expression for $DDSRES(i)$ can be obtained, as shown in Equation (32).

$$DDSRES(ij) = \overline{T_{ij}(DD)}, \tag{32}$$

Wherein, all functions are in units of seconds.

Let the buffer time be B_{ij}, and let the departure separation be M_{ij} as specified in the relevant flight rule. Then, the expression for $T_{ij}(DD)$ and $\overline{T_{ij}(DD)}$ can be obtained, as shown in Equations (33) and (34).

$$T_{ij}(DD) = M_{ij} + B_{ij} + e_0, \tag{33}$$

$$\overline{T_{ij}(DD)} = M_{ij} + B_{ij}, \tag{34}$$

Wherein, all functions are in units of seconds.

When $T_{ij}(DD) < M_{ij}$ occurs, the flight safety separation regulations are violated. Let the probability that successive departing aircraft meet the flight safety separation regulations be p_c. In a simplified calculation process, the expression for the buffer time B_{ij} can be obtained, as shown in Formula (35).

$$B_{ij} = \sigma_0\Phi^{-1}(p_c), \tag{35}$$

Wherein, the unit of B_{ij} is seconds.

The expression for successive departing aircraft time separation regulations is as shown in Formula (36).

$$DDSRES(ij) = \overline{T_{ij}(DD)} = M_{ij} + \sigma_0\Phi^{-1}(p_c), \tag{36}$$

Wherein, the unit of $DDSRES(ij)$ is seconds.

4.3.4. General Aviation Airport Single Runway Departure Capacity

According to Formulas (1) and (2), and the derivation results from Sections 4.3.2 and 4.3.3, the expression for the single runway departure capacity of general aviation airports under the VFR and IFR can be obtained, as shown in Formula (37).

$$C_{VFR/IFR}(DD) = \frac{1}{\sum_{i=1}^{n}\sum_{j=1}^{n} p_{ij}\left[\max\left(DRORES(i)_{VFR/IFR} \quad DDSRES(ij)_{VFR/IFR}\right)\right]}, \tag{37}$$

Wherein, $C_{VFR/IFR}(DD)$ represents the single runway departure capacity under the VFR or IFR, its unit is sorties per hour; p_{ij} represents the probability that the preceding aircraft is type i and the following aircraft is type j; $p_{ij} = p_i \cdot p_j$, $p_{ij} > 0$, $\sum_{i=1}^{n}\sum_{j=1}^{n} p_{ij} = 1$.

This is similar to the analysis in Section 4.2.4. Therefore, the expression for the single runway departure capacity of general aviation airports can be obtained, as shown in Formula (38).

$$C(DD) = \sum_{i=1}^{n}\sum_{j=1}^{n} p_{ij_{VFR}} C_{VFR}(DD) + \left(1 - \sum_{i=1}^{n}\sum_{j=1}^{n} p_{ij_{VFR}}\right) C_{IFR}(DD), \tag{38}$$

Wherein, $C(DD)$ represents the single runway departure capacity of a general aviation airport, its unit is sorties per hour; $p_{ij_{VFR}}$ represents the proportion that successive departing aircraft i and j both takeoff according to the VFR.

4.4. General Aviation Airport Single Runway Mixed Capacity Evaluation Model

4.4.1. General Aviation Airport Single Runway Mixed Capacity Analysis

In a mixed operation mode, it is usually necessary to have sufficient idle time between arriving aircraft before releasing departing aircraft. Based on the above analysis, the matrix expression for the runway idle time I_{ij} between successive arriving aircraft is shown in Equation (39).

$$\left[I_{ij}\right]_{n\times n} = \left[T_{ij}(AA)\right]_{n\times n} - \left[ARORES(i)\right]_{n\times 1}\begin{bmatrix}1 & \cdots & 1\end{bmatrix}_{1\times n}, \tag{39}$$

Wherein, $T_{ij}(AA)$ represents the time separation between successive arriving aircraft in a mixed operation mode, its unit is seconds; n represents the number of aircraft types.

Considering the impact of factors such as the number of aircraft that can be released between successive arriving aircraft, the average time interval between successive departing aircraft, and the time separation between the last departing aircraft and the arriving aircraft on the runway, the expression for the runway idle time R_{ij}^{m} can be obtained, as shown in Formula (40).

$$\begin{aligned}&\left[R_{ij}^{m}\right]_{n\times n} = \\ &\left[I_{ij}\right]_{n\times n} - (m_{ij}-1)\begin{bmatrix}1 & \cdots & 1\end{bmatrix}_{1\times n}^{T}\left[E\left(DDSRES_{i^*j^*}\right)\right]\begin{bmatrix}1 & \cdots & 1\end{bmatrix}_{1\times n} - \begin{bmatrix}1 & \cdots & 1\end{bmatrix}_{1\times n}^{T}\left[DASRES_{i^{**}j}\right]\begin{bmatrix}1 & \cdots & 1\end{bmatrix}_{1\times n}\end{aligned}, \tag{40}$$

Wherein, $E\left(DDSRES_{i^*j^*}\right)$ represents the average time separation between successive departing aircraft under different departure methods, its unit is seconds; $DASRES_{i^{**}j}$ represents the time separation between the last departing aircraft and the arriving aircraft, its unit is seconds; when R_{ij}^{m} takes a negative value, the corresponding m is the maximum number of aircraft that can be released.

After obtaining the maximum release number m, it is possible to determine the number of departing and arriving aircraft that the runway can serve, and after processing, the corresponding mixed operation capacity can be obtained. It can be seen that the key parameters in this model are $E\left(DDSRES_{i^*j^*}\right)$ and $DASRES_{i^{**}j}$. As indicated in Section 4.3, the derivation process of these parameters in the two flight rules is essentially the same. Therefore, a unified derivation is conducted here for the single runway mixed capacity evaluation model of general aviation airports under the VFR and IFR.

4.4.2. Successive Departing Aircraft Average Time Separation

As introduced in Sections 2.2 and 2.3, the departing procedures under the VFR and IFR include direct departure and turning departure. The different departure methods correspond to different safety separations. Therefore, the expression for $E\left(DDSRES_{i^*j^*}\right)$ is shown in Formula (41).

$$E\left(DDSRES_{i^*j^*}\right) = p_{DD}\sum_{i^*=1}^{n}\sum_{j^*=1}^{n} p_{i^*j^*} DDSRES_{i^*j^*} + p_{TD}\sum_{i^*=1}^{n}\sum_{j^*=1}^{n} p_{i^*j^*} DDSRES^{*}_{i^*j^*}, \tag{41}$$

Wherein, $DDSRES_{i^*j^*}$ represents the time separation regulation for direct departure aircraft, its unit is seconds; $DDSRES^*_{i^*j^*}$ represents the time separation regulation for turning departure, its unit is seconds; p_{DD} represents the proportion of direct departure aircrafts; and p_{TD} represents the proportion of turning departure aircrafts; $p_{DD} + p_{TD} = 1$.

4.4.3. Departing and Arriving Aircraft Time Separation Regulation

Let the time separation $T_{ij}(DA)$ between departing and arriving aircraft be a random variable, and $T_{ij}(DA) \sim N\left(\overline{T_{ij}(DA)}, \sigma_0^2\right)$. In the absence of random errors, the expression for $DASRES(i)$ can be obtained, as shown in Equation (42).

$$DASRES(ij) = \overline{T_{ij}(DA)}, \tag{42}$$

Wherein, all functions are in units of seconds.

Let the buffer time be B_{ij}, and the departure separation M_{ij} as specified in the relevant flight rule. Then, the expression for $T_{ij}(DA)$ and $\overline{T_{ij}(DA)}$ can be obtained, as shown in Equations (43) and (44).

$$T_{ij}(DA) = M_{ij} + B_{ij} + e_0, \tag{43}$$

$$\overline{T_{ij}(DA)} = M_{ij} + B_{ij}, \tag{44}$$

Wherein, the unit for all functions, except for the random variable e_0, is seconds.

Assuming that under the premise of flight safety, the minimum distance δ_d that the arriving aircraft reaches from the entrance of the RES, and the flight speed of the departing aircraft i is V_i, the expression for M_{ij} can be obtained, as shown in Equation (45).

$$M_{ij} = \frac{\delta_d}{v_i}, \tag{45}$$

Wherein, the unit of δ_{ij} is meters, the unit of v_i is meters per second, and the unit of M_{ij} is seconds.

When $T_{ij}(DA) < M_{ij}$ occurs, the flight safety separation regulations are violated. Let the probability that departing and arriving aircraft meet the flight safety separation regulations be p_c. In a simplified calculation process, the expression for the buffer time B_{ij} can be obtained, as shown in Formula (46).

$$B_{ij} = \sigma_0 \Phi^{-1}(p_c), \tag{46}$$

Wherein, the unit of B_{ij} is seconds.

The expression for departing and arriving aircraft time separation regulations is as shown in Formula (47).

$$DASRES(ij) = \overline{T_{ij}(DA)} = \frac{\delta_d}{v_i} + \sigma_0 \Phi^{-1}(p_c), \tag{47}$$

Wherein, the unit of $DASRES(ij)$ is seconds.

4.4.4. General Aviation Airport Single Runway Mixed Capacity

The mixed capacity of the runway should be determined by the arriving capacity and the maximum number of aircraft that can be released in the mixed operation mode. Therefore, the mixed capacity evaluation model for a single runway in general aviation airports under the VFR and IFR is shown in Formula (48).

$$C_{VFR/IFR}(DA) = C_{VFR/IFR-A}(DA)\left(1 + \sum_{i=1}^{n}\sum_{j=1}^{n} p_{ij} m_{ij\max}\right) = \frac{1 + \sum\limits_{i=1}^{n}\sum\limits_{j=1}^{n} p_{ij} m_{ij\max}}{\sum\limits_{i=1}^{n}\sum\limits_{j=1}^{n} p_{ij} T_{ij}(AA)}, \tag{48}$$

Wherein, $C_{VFR/IFR-A}(DA)$ represents the landing capacity in the mixed operation mode of the VFR and IFR, its unit is sorties per hour; $\sum_{i=1}^{n}\sum_{j=1}^{n} p_{ij}m_{ij\max}$ represents the average number of aircraft that can be released.

To ensure flight safety, the safety separation between departing and arriving aircraft in the mixed operation mode should be configured according to the same flight rule. Therefore, the mixed capacity evaluation model for a single runway in general aviation airports can be obtained, as shown in Formula (49).

$$C(DA) = P_{VFR}C_{VFR}(DA) + P_{IFR}C_{IFR}(DA), \tag{49}$$

Wherein, $C(DA)$ represents the mixed capacity of a single runway at a general aviation airport, its unit is sorties per hour; P_{VFR} represents the proportion of VFR; P_{IFR} represents the proportion of IFR; $P_{VFR} > 0$, $P_{IFR} > 0$, $P_{VFR} + P_{IFR} = 1$.

5. Analysis of Runway Capacity Assessment Examples for General Aviation Airports

5.1. Factor Analysis

According to public information from the Aircraft Owners and Pilots Association of China, a certain airport is selected as the sample airport. This airport is an A1 category runway-type general aviation airport, with runways numbered 17–35. Each runway is 1200 m long and 30 m wide and equipped with four taxiways. Taxiways 1 and 4 are rapid link taxiways, located 300 m from the ends of runways 17 and 35, respectively, while taxiways 2 and 3 are common link taxiways, located 500 m from the ends of runways 17 and 35, respectively. Aircraft can use visual and instrument flight procedures for arrival and departure based on weather conditions. The flight procedures for arrival and departure are shown in Figure 11.

When weather conditions permit the VFR, aircraft use the left traffic pattern below an altitude of 1000 m for arrivals. The lengths of the airport's left traffic pattern are as follows: the departure leg and crosswind leg are 3 km, the base leg is 3 km, and for the left short approach, the departure leg is 1 km and the final approach is 2 km. When taking off from Runway 17, aircraft heading to point Alpha should join the left traffic pattern or the left short approach after takeoff and climb to the corresponding altitude before heading out. Aircraft heading to other points should climb to the specified altitude after takeoff and then make a left or right turn to head out. When taking off from Runway 35, aircraft must climb to the specified altitude and then make a left or right turn to head out.

When weather conditions permit the IFR, for aircraft landing on Runway 17, those entering at point Alpha should join the IF for direct landing, those entering at point Beta should join the teardrop pattern procedure for landing, and those entering at point Delta should join the straight-in penetration procedure for landing. For aircraft landing on Runway 35, those entering at point Alpha should join the teardrop pattern procedure for landing, those entering at point Beta should join the racetrack for landing, and those entering at point Delta should join the IF for direct landing. For departure, aircraft must climb to the specified altitude and then make a left or right turn to head out.

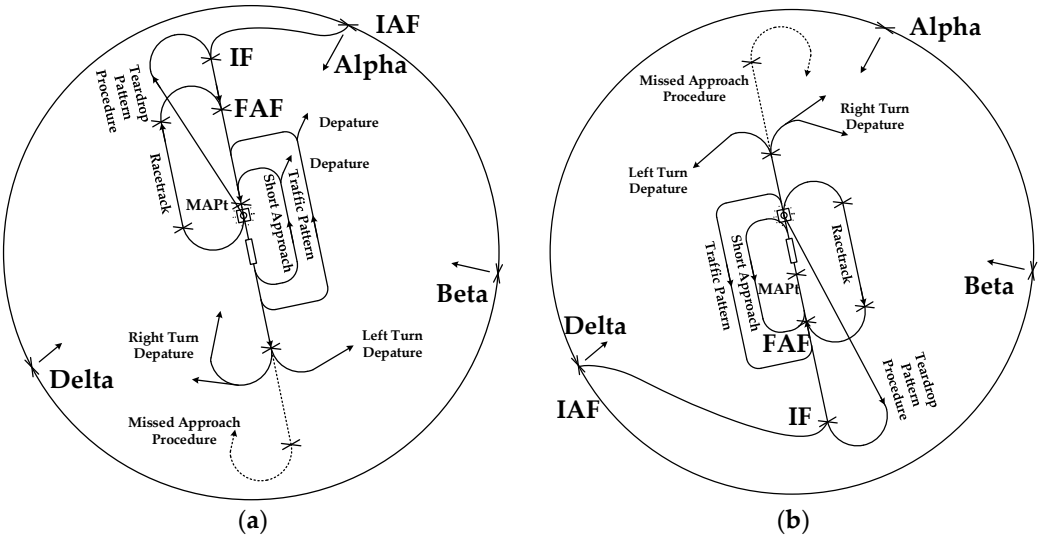

Figure 11. Arrival and departure procedures for a certain airport. (**a**) Arrival and departure procedures for Runway 17. (**b**) Arrival and departure procedures for Runway 35.

5.2. Case Evaluation

To facilitate modeling and analysis, the access points of the VFR-RES are consistent with those in Section 3.1. For the IFR-RES, for aircraft using the teardrop pattern procedure for landing, the IAF is selected as the starting point of the public approach lane, and the IF is the RES entry. For aircraft using the racetrack for landing, the IAF is selected as the starting point of the public approach lane, and the FAF is the entrance to the RES entry, with the exit being consistent with Section 3.2. Flight safety separation is configured according to the general standards of procedural control. Combined with the relevant statistical data of the airport, the runway capacity evaluation parameters are given as shown in Table 1 below.

Table 1. Single Runway Capacity Evaluation Parameters for a Certain Airport.

	Parameter Type	Aircraft 1	Aircraft 2	Aircraft 3
Performance Parameters	Arrival speed (km/h)	200	180	245
	Departure speed (km/h)	120	120	100
	Landing distance (m)	200	180	230
RES parameters	Aircraft exit speed (km/h)		20	
	Length of public approach lane (km)		15	
	VFR: Distance from RES Entry to Runway (km)		3	
	Racetrack: Distance from RES Entry to Runway (km)		5	
	Teardrop pattern procedure: Distance from RES Entry to Runway (km)		6	
	Short approach flight time (s)		80	
	Traffic pattern final approach flight time (s)		130	
	Teardrop pattern procedure flight time (s)		180	
	Racetrack flight time (s)		150	
	Direct departure time (s)		VFR: 60 IFR: 70	
	Turning departure time (s)		VFR: 70 IFR: 80	
Safety separation parameters	VFR: Minimum safe landing separation (km)		1	
	IFR: Minimum safe landing separation (min)		3	
	VFR: Minimum safe takeoff separation (min)		1.5	
	IFR: Minimum safe takeoff separation (min)		2	

Table 1. *Cont.*

	Parameter Type	Aircraft 1	Aircraft 2	Aircraft 3
Other parameters	Aircraft type probability (%)	40	35	25
	Not violating air traffic control rules probability (%)		0.95	
	Selecting a rapid link taxiway probability (%)		60	
	Selecting a common link taxiway probability (%)		40	
	Direct departure probability (%)		70	
	Turning departure probability (%)		30	
	VFR probability %		75	
	IFR probability %		25	

It is important to note that during subsequent calculations, the data in the above table should be converted into the appropriate units. To accelerate the arrival and departure speed, under the VFR, aircraft 1 and 2 are instructed to land on the short approach, and under the IFR, aircraft 1 is directed to join the teardrop pattern procedure for IF landing, while aircraft 2 and 3 are to join the racetrack for landing. Assume that the probabilities of aircraft choosing the two rapid link taxiways are 70% and 30%, respectively, and the probabilities of choosing the two common link taxiways are 80% and 20%, respectively. After calculation, the single runway capacity assessment results for the general aviation airport are presented in Table 2.

Table 2. Evaluation results of the single runway capacity of a general aviation airport.

Operation Mode	Capacity (sorties/hour)	Total	Capacity (sorties/hour)
VFR arrival capacity IFR arrival capacity	12 9	Single runway arrival capacity	12
VFR departure capacity IFR departure capacity	21 18	Single runway departure capacity	21
VFR mixed capacity IFR mixed capacity	21 12	Single runway mixed capacity	21

5.3. Numerical Experiment

5.3.1. Impact of Flight Rules on Runway Capacity

Keeping the parameters in Table 1 constant and changing the proportion of aircraft using different flight rules, a trend graph of runway capacity variation with flight rules can be obtained, as shown in Figure 12.

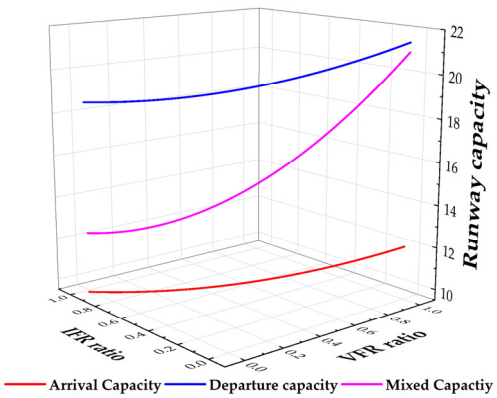

Figure 12. Runway capacity variation with flight rules.

As shown in the figure, with the increasing proportion of aircraft using the VFR, the single runway arrival capacity, departure capacity, and mixed capacity of general aviation

airports are all improving. Among them, the arrival capacity values are relatively low, which is because the time aircraft spend using the RES for landing is more than that for takeoff, resulting in the arrival capacity being less than the departure capacity. In summary, the experimental results are in line with the actual flight operations of general aviation airports and verify the reliability of the established model.

5.3.2. Impact of Flight Procedures on Runway Capacity

Keeping the parameters in Table 1 constant and altering the proportion of aircraft using different arrival and departure procedures under various flight rules, a trend graph of runway capacity variation with flight procedures can be obtained, as shown in Figure 13.

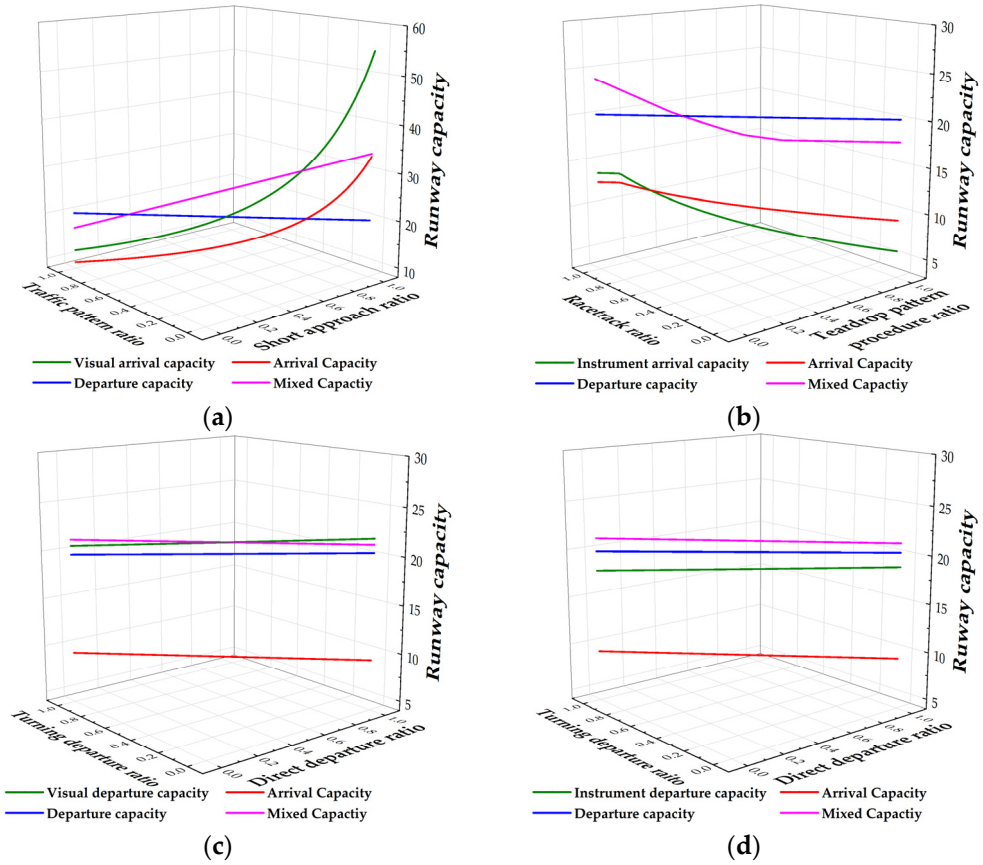

Figure 13. Runway capacity variation with flight procedures. (**a**) Effect of visual approach procedure on runway capacity; (**b**) Effect of instrument approach procedure on runway capacity; (**c**) Effect of visual departure procedure on runway capacity; (**d**) Effect of instrument departure procedure on runway capacity.

As can be seen from Figure 13a,b, with other parameters remaining constant, as the proportion of aircraft using short approach and teardrop pattern procedure programs increases, the corresponding VFR arrival capacity, IFR arrival capacity, and arrival capacity are continuously increasing. This is because, according to factor analysis, the use of short approach and teardrop pattern procedures during landing helps to accelerate the aircraft's landing speed, thereby further increasing the arrival capacity. As can be seen from Figure 13c,d, with other parameters remaining constant, the choice of different departure routes under the VFR and IFR has a relatively small impact on capacity. According to the data in Table 1, the difference in departure times under different flight rules during departure is small, hence the impact on capacity is also relatively small. In conclusion, the experimental results verify the important role of the short approach in accelerating arrival and departure speeds and improving the operational efficiency of airports.

5.3.3. Impact of Flight Separation on Runway Capacity

Keeping the performance parameters, RES parameters, and other parameters in Table 1 constant, and altering the safety separation parameters, a trend graph of runway capacity variation with flight separation can be obtained, as shown in Figure 14.

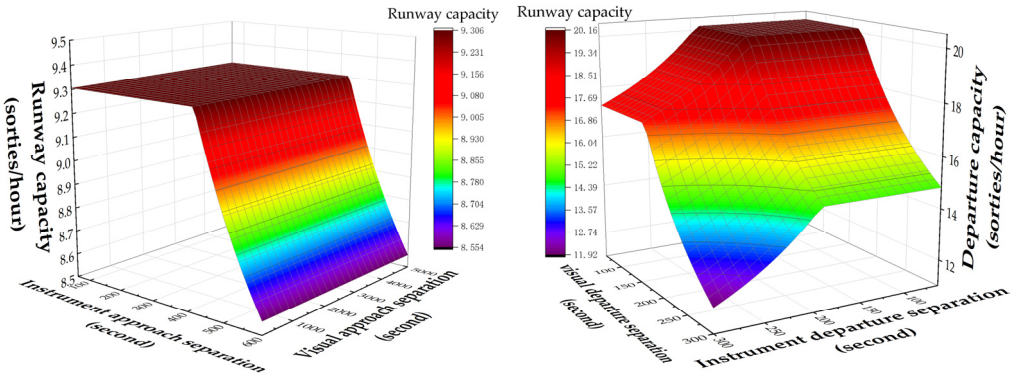

(**a**) (**b**)

Figure 14. Runway capacity variation with flight separation. (**a**) Arrival capacity variation with flight separation; (**b**) Departure capacity variation with flight separation.

As can be seen from Figure 14a, in the case of arrival, the arrival capacity is not affected by the VFR approach separation, but it shows a stable trend as the IFR approach separation increases. This is because, during the process of maintaining a higher approach speed, the actual arrival time is less than the time occupied by the RES. Therefore, under this experimental condition, the runway capacity shows a stable trend. In the instrument landing process, the runway capacity remains stable when the separation between successive arriving aircraft is less than the time occupied by the RES. However, when the separation between successive arriving aircraft is greater than the time occupied by the RES, the time spent serving IFR approach aircraft on the runway will increase, resulting in a continuous decrease in arrival capacity. As can be seen from Figure 14b, the departure capacity decreases as the VFR and IFR departure separation increases. This is because when the separation between successive departure aircraft under both flight rules is greater than the time occupied by the RES, the time spent serving departure aircraft under both flight rules will increase, leading to a continuous decrease in arrival capacity. In conclusion, the experimental results verify that the RES can ensure the stability of general aviation airport capacities under certain conditions.

5.3.4. The Impact of Aircraft Departure Runway Strategy on Runway Capacity

(1) The impact of arriving aircraft choosing different taxiways to exit the runway on runway capacity

Keeping the performance parameters, RES parameters, and safety separation parameters in Table 2 unchanged, and controlling the proportion of aircraft choosing rapid link taxiways 1 and 4, as well as common link taxiways 2 and 3, both at 0.5, by altering the proportion of aircraft selecting rapid link taxiways versus common link taxiways, a trend graph of runway capacity changes with the selection of different taxiways for exiting the runway by arriving aircraft can be obtained, as shown in Figure 15.

As can be seen from Figure 15, it can be seen that as the proportion of aircraft using rapid link taxiways to leave the runway continues to increase, the landing capacity and mixed capacity of the general aviation airport's single runway show a slow upward trend, while the departure capacity remains stable. This is because the difference in runway occupancy time between using rapid link taxiways and common link taxiways is relatively small. As the proportion of aircraft using rapid link taxiways to leave the runway increases, the trend of capacity improvement is still relatively flat. There is a jump in the mixed

capacity in the figure. Although the arrival capacity increases at the point of the jump curve, the idle time between the two successive arriving aircraft does not meet the minimum time interval required for a departure aircraft, preventing the aircraft from taking off. Only when the arrival capacity continues to increase and the idle time between two successive arriving aircraft is sufficient to accommodate an additional takeoff aircraft will the mixed capacity stabilize again.

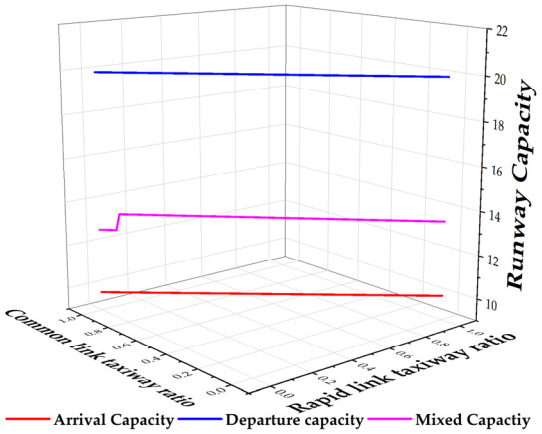

Figure 15. Trend of runway capacity variation as arriving aircraft select different connecting taxiways to leave the runway.

(2) The impact of arriving aircraft choosing the nth rapid link taxiway on runway capacity

Keeping the performance parameters, RES parameters, and safety separation parameters in Table 2 unchanged, and controlling the proportion of aircraft choosing rapid link taxiways and common link taxiways both at 0.5, with the proportion of aircraft choosing common link taxiways 2 and 3 also at 0.5 for both taxiways, and with the landing direction at 170°, the trend of runway capacity as the arriving aircraft select the nth rapid link taxiway to leave the runway is shown in Figure 16.

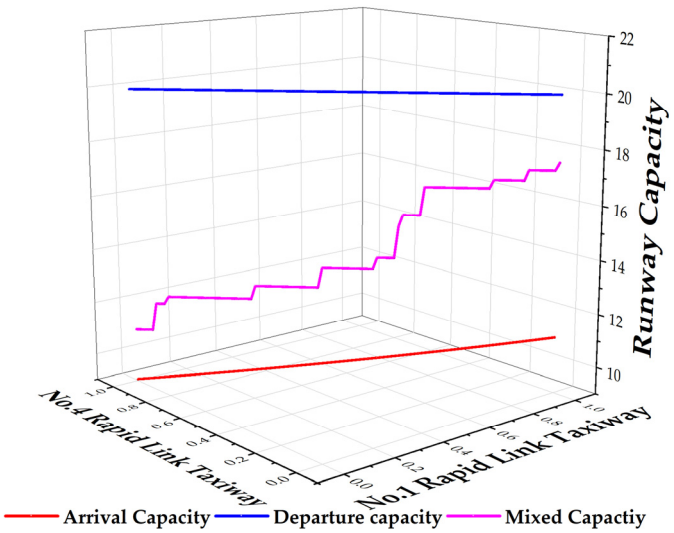

Figure 16. The trend of runway capacity as arriving aircraft select the nth rapid link taxiway to depart the runway.

As shown in the figure, with the increasing proportion of aircraft using the No. 1 rapid link taxiway to leave the runway, both the single runway arrival capacity and the mixed capacity of general aviation airports show an upward trend, while the departure capacity remains stable. This is because when aircraft use the No. 1 rapid link taxiway to leave the

runway, the runway occupancy time is shorter, leading to an upward trend in capacity improvement. The mixed capacity experiences multiple jumps, and the basic reasons are similar to those analyzed in point (1), so they are not detailed here. It is worth noting that the use of rapid link taxiways by arriving aircraft can more quickly increase runway capacity, so in the above figure, the mixed capacity shows the fastest increase among the three sets of experiments.

(3) The impact of arriving aircraft choosing the nth rapid link taxiway on runway capacity

Keeping the performance parameters in Table 2, the RES parameters, and the safety interval parameters constant, and controlling the proportion of aircraft choosing rapid link taxiways and common link taxiways both at 0.5, as well as the proportion choosing rapid link taxiway No. 1 and No. 4 both at 0.5, with a landing direction of 170°, the trend of runway capacity as the arriving aircraft select the nth common link taxiway to leave the runway is shown in Figure 17.

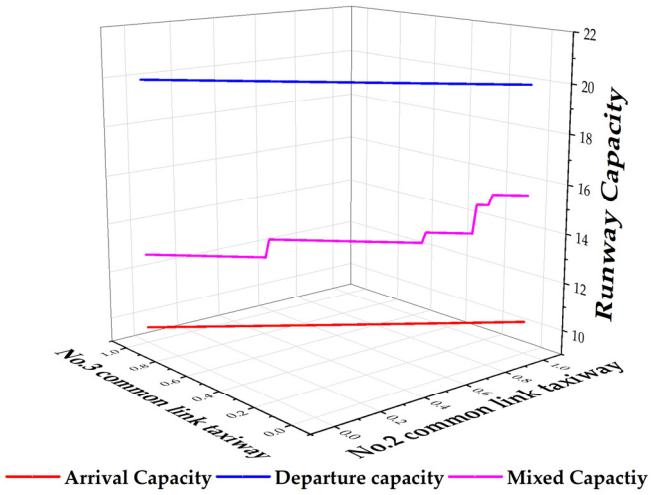

Figure 17. The trend of runway capacity as arriving aircraft select the nth common link taxiway to depart the runway.

From the figure, it can be seen that as the proportion of aircraft using the No. 2 rapid link taxiway to leave the runway continues to increase, both the single runway arrival capacity and the mixed capacity of the general aviation airport show an upward trend, while the departure capacity remains stable. This is because when aircraft use the No. 2 common link taxiway to leave the runway, the runway occupancy time is shorter, leading to an upward trend in capacity improvement. Due to the short distance between the two common taxiways, the runway occupancy time for aircraft using the two common link taxiways differs slightly, so the upward trend in landing capacity here is slower than that in Figure 16.

The above indicates that the capacity assessment results obtained from different departure strategies are consistent with the actual flight operations at general aviation airports, once again verifying the objective feasibility of the model established in this paper.

6. Conclusions

To further enhance the operational management capabilities of general aviation airports and better meet the increasing demand for flight traffic, this study focuses on relevant general aviation airports in China. Based on the operational characteristics of general aviation airports under visual and instrument flight rules, the concept of a RES is introduced. By combining this concept with a spatiotemporal analysis model, a new runway capacity assessment model for general aviation airports is constructed. This model encompasses various operational modes such as arrival, departure, and mixed operations, providing a more comprehensive evaluation method for general aviation airports. Moreover, numerical

experiments that include factors such as flight rules, flight procedures, flight spacing, and departure strategies have been designed to further validate the rationality and reliability of the proposed model, offering new perspectives and methods for related research.

Overall, the main contributions of this paper are as follows:

(1) This paper proposes a new concept of the RES. In order to improve the operational management capabilities of general aviation airports, this study focuses on the evaluation of runway capacity. Based on the flight rules and procedures of general aviation airports, and in accordance with the critical mutual exclusion rule and the flight safety requirements for aircraft arrival and departure, a Runway Extension System for general aviation airports is established. This system expands the connotation and scope of the runway in both time and space. Compared to traditional assessment models that only consider the runway, this approach is more precise. It provides a fundamental theoretical framework for subsequent research, which can be further improved and expanded upon.

(2) This paper provides a new approach and method for the evaluation of runway capacity at general aviation airports. In constructing the runway capacity assessment model, the actual procedural control of general aviation airports is fully considered, and a RES is established that differentiates between Visual Flight Rules and Instrument Flight Rules. From a new perspective, a novel method for runway capacity assessment research is proposed that is suitable for most general aviation airports. Compared to traditional assessment methods, the method proposed in this paper is more in line with the operational characteristics of the majority of general aviation airports in China. Additionally, it has good scalability and can be adjusted and improved according to the differences of various airports.

(3) A model reference is provided for the runway capacity of general aviation airports. Based on the proposed runway extension system, this paper improves the traditional space–time analysis model to better align with the actual runway capacity assessment of general aviation airports. It can better reflect the actual arrival, departure, and mixed operation scenarios of different aircraft combinations at general aviation airports. The calculation results can provide model and data support for the operational management of related general aviation airports.

In addition, this paper conducts relevant case evaluations and numerical experiments to verify the reliability and rationality of the proposed model. However, in this research, the process of aircraft arrival and departure is simplified as a simple follow-up activity. In subsequent research, factors such as visibility, wind speed, and other related factors should be considered and incorporated into the model to further improve the accuracy of the capacity assessment results.

Author Contributions: Ideas, Z.C., H.X. and B.H.; method, Z.C., H.X. and B.H.; software, Z.C. and Y.S.; data curation, T.Z. and F.Z.; writing—original draft preparation, Z.C.; writing—review and editing, H.X. and B.H. All authors have read and agreed to the published version of the manuscript.

Funding: This research received no external funding.

Data Availability Statement: The numerical simulation data used to support the findings of this study are included within the article.

Acknowledgments: The authors are thankful to anonymous reviewers for their instructive reviewing of the manuscript.

Conflicts of Interest: Author Bangcun Han was employed by the company Shandong Airport Management Group Rizhao Airport Co., Ltd. The remaining authors declare that the research was conducted in the absence of any commercial or financial relationships that could be construed as a potential conflict of interest.

References

1. Civil Aviation Administration of China. Statistical Bulletin of Civil Aviation Industry Development in 2023. Available online: https://www.caac.gov.cn/English/News/202406/t20240627_224599.html (accessed on 27 June 2024).
2. Bowen, E.G.; Pearcey, T. Delays in the Flow of Air Traffic. *J. R. Aeronaut. Soc.* **1948**, *52*, 251–258. [CrossRef]
3. Xiao, Y.B.; Fu, X.W.; Oum, T.H.; Yan, J. Modeling Airport Capacity Choice with Real Options. *Transp. Res. B Methodol.* **2017**, *100*, 93–114. [CrossRef]
4. Wang, S.J.; Yang, B.T.; Duan, R.R.; Li, J.H. Predicting the Airspace Capacity of Terminal Area under Convective Weather Using Machine Learning. *Aerospace* **2023**, *10*, 288. [CrossRef]
5. Ren, J.; Qu, S.R.; Wang, L.L.; Wang, Y.; Lu, T.T.; Ma, L.J. Research on En Route Capacity Evaluation Model based on Aircraft Trajectory Data. *Electron. Res. Arch.* **2023**, *31*, 1673–1690. [CrossRef]
6. Chang, Y.H.; Solak, S.; Clarke, J.P.B.; Johnson, E.L. Models for Single-sector Stochastic Air Traffic Flow Management Under Reduced Airspace Capacity. *J. Oper. Res. Soc.* **2016**, *67*, 54–67. [CrossRef]
7. Zhang, M.; Shan, L.; Liu, K.; Yu, H.; Yu, J. Terminal Airspace Sector Capacity Estimation Method Based on The ATC Dynamical Model. *Kybernetes* **2016**, *45*, 884–899. [CrossRef]
8. Mascio, P.D.; Rappoli, G.; Moretti, L. Analytical Method for Calculating Sustainable Airport Capacity. *Sustainability* **2020**, *12*, 9239. [CrossRef]
9. Federal Aviation Administration. *Airport Capacity and Delay*; AC: 150/5060-5; U.S. Department of Transportation, Federal Aviation Administration: Washington, DC, USA, 1983. Available online: https://www.faa.gov/documentLibrary/media/Advisory_Circular/150_5060_5.pdf (accessed on 5 November 2020).
10. Mitkas, D.Z.; Lovell, D.J.; Young, S.B.; Venkatesh, S. Developing Capacity Estimation Metrics for Airports Accommodating Smaller Aircraft Using Locally Collected Automated Dependent Surveillance-Broadcast Data. *Transp. Res. Rec.* **2022**, *2676*, 285–295. [CrossRef]
11. Farhadi, F.; Ghoniem, A.; Al-Salem, M. Runway Capacity Management—An Empirical Study with Application to Doha International Airport. *Transp. Res. Part E Logist. Transp. Rev.* **2014**, *68*, 53–63. [CrossRef]
12. Ng, K.K.H.; Lee, C.K.M.; Zhang, S.Z.; Keung, K.L. The Impact of Heterogeneous Arrival and Departure Rates of Flights on Runway Configuration Optimization. *Int. J. Transp. Res.* **2021**, *14*, 215–226. [CrossRef]
13. Du, W.B.; Chen, S.W.; Li, H.T.; Li, Z.S.; Cao, X.B.; Lv, Y.S. Airport Capacity Prediction With Multisource Features: A Temporal Deep Learning Approach. *IEEE Trans. Intell. Transp. Syst.* **2023**, *24*, 615–630. [CrossRef]
14. Donmez, K.; Aydogan, E.; Cetek, C.; Maras, E.E. The Impact of Taxiway System Development Stages on Runway Capacity and Delay Under Demand Volatility. *Aerospace* **2023**, *10*, 6. [CrossRef]
15. Shen, Z.Y.; Xu, X.Y.; He, Y.; Yan, Y.G.; Zhou, L.; Hu, Y.Y. An Improved Runway Operation Capacity Model for V-open Multirunway Airports in China. *J. Adv. Transp.* **2022**, *2022*, 5869101. [CrossRef]
16. Maltinti, F.; Flore, M.; Pigozzi, F.; Coni, M. Optimizing Airport Runway Capacity and Sustainability through the Introduction of Rapid Exit Taxiways: A Case Study. *Sustainability* **2024**, *16*, 5359. [CrossRef]
17. Gao, H.R.; Xie, Y.B.; Yuan, C.J.; He, X.; Niu, T.T. Prediction of Aircraft Arrival Runway Occupancy Time Based on Machine Learning. *Int. J. Comput. Intell. Syst.* **2023**, *16*, 150. [CrossRef]
18. Janic, M. Modeling Effects of Different Air Traffic Control Operational Procedure, Separation Rules, and Service Disciplines on Runway arrive Capacity. *J. Adv. Transp.* **2014**, *48*, 556–574. [CrossRef]
19. Kim, A.; Rokib, S.A.; Liu, Y. Refinements to a Procedure for Estimating Airfield Capacity. *Transp. Res. Rec.* **2015**, *2501*, 18–24. [CrossRef]
20. Sekine, K.; Kato, F.; Kageyama, K.; Itoh, E. Data-Driven Simulation for Evaluating the Impact of Lower Arrival Aircraft Separation on Available Airspace and Runway Capacity at Tokyo International Airport. *Aerospace* **2021**, *8*, 165. [CrossRef]
21. Sznajderman, L.; Ramírez-Díaz, G.; Di Bernardi, C.A. Influence of the Apron Parking Stand Management Policy on Aircraft and Ground Support Equipment (GSE) Gaseous Emissions at Airports. *Aerospace* **2021**, *8*, 87. [CrossRef]
22. Tee, Y.Y.; Zhong, Z.W. Modelling and Simulation Studies of the Runway Capacity of Changi Airport. *Aeronaut. J.* **2018**, *122*, 1022–1037. [CrossRef]
23. Cetek, C.; Cinar, E.; Aybek, F.; Cavcar, A. Capacity and Delay Analysis for Airport Manoeuvring Areas using Simulation. *Aircr. Eng. Aerosp. Technol.* **2014**, *86*, 43–55. [CrossRef]
24. Yang, P.; Gao, W.; Sun, J.Q. Capacity Analysis for Parallel Runway Through Agent-Based Simulation. *Math. Probl. Eng.* **2013**, *2013*, 505794.
25. Díaz, M.V.; Comendador, F.G.; Carretero, J.G.H.; Valdés, R.M.A. Analyzing the Departure Runway Capacity Effects of Integrating Optimized Continuous Climb Operations. *Int. J. Aerosp. Eng.* **2019**, *2019*, 3729480.
26. Kaplan, Z.; Çetek, C. A Monte Carlo approach for capacity and delay analyses of multiple interacting airports in Istanbul metroplex. *Aeronaut. J.* **2024**, *128*, 1935–1960. [CrossRef]
27. Wan, L.L.; Peng, Q.P.; Tian, Y.; Gao, L.; Ye, B.J. Airport Capacity Evaluation Based on Air Traffic Activities Big Data. *EURASIP J. Wirel. Commun. Netw.* **2020**, *2020*, 227. [CrossRef]
28. Starita, S.; Strauss, A.K.; Fei, X.; Jovanovic, R.; Ivanov, N.; Pavlovic, G.; Fichert, F. Air Traffic Control Capacity Planning Under Demand and Capacity Provision Uncertainty. *Transp. Sci.* **2020**, *54*, 882–896. [CrossRef]

29. Kuennen, J.R.; Strauss, A.K.; Ivanov, N.; Jovanovi, R.; Fichert, F.; Starita, S. Cross-Border Capacity Planning in Air Traffic Management Under Uncertainty. *Transp. Sci.* **2023**, *57*, 839–1114. [CrossRef]
30. Gao, S.; Wang, L. How Flight Experience Impacts Pilots' Decision-making and Visual Scanning Pattern in Low-visibility Approaches: Preliminary Evidence From Eye Tracking. *Ergonomics* **2024**, *67*, 1284–1300. [CrossRef]
31. Romanovic, R.; Samardzic, K.; Novak, D. Prerequisites for Statistical Analyses of the Quality of Instrument Flight Procedures. *Promet-Traffic Transp.* **2024**, *36*, 203–218. [CrossRef]
32. Cai, L.C.; Shao, B.; Zheng, R.H.; Chong, X.L. Determining method of airfield clearance zone. *J. Traffic Transp. Eng.* **2004**, *4*, 40–43.
33. Hunan Huaxing General Aviation Co., Ltd. *Changsha Kaihui Airport Flight Procedure*; Hunan Huaxing General Aviation Co., Ltd.: Changsha, China, 2019; pp. 2–3.
34. Sun, H.; Zhou, X.; Zhang, P.W.; Liu, X.; Lu, Y.S.; Huang, H.; Song, W.Y. Competency-based assessment of pilots' manual flight performance during instrument flight training. *Cogn. Technol. Work.* **2023**, *25*, 345–356. [CrossRef]
35. International Civil Aviation Organization. Construction of Visual and Instrument Flight Procedures. Available online: https://skybrary.aero/bookshelf/doc-8168-volume-ii-construction-visual-and-instrument-flight-procedures-sixth-addition (accessed on 13 November 2014).